

Electronic Supplementary Information

Novel one-step gas-phase reaction synthesis of transition metal sulfide nanoparticles embedded in carbon matrices for reversible lithium storage

Peili Lou^{a,b}, Yingbin Tan^a, Ping Lu^a, Zhonghui Cui^{a,*} and Xiangxin Guo^{a,*}

^a State Key Laboratory of High Performance Ceramics and Superfine Microstructure, Shanghai Institute of Ceramics, Chinese Academy of Sciences, Shanghai 200050 China.

*E-mail: cuizhognhui@mail.sic.ac.cn (Z. H. Cui), xxguo@mail.sic.ac.cn (X. X. Guo)

^b University of Chinese Academy of Sciences, Beijing 100039 China.

Experimental section

Synthesis of TMS@C nanocomposites The reagents were obtained from Alfa Aesar and used as received. To synthesize the TMS@C nanocomposites, the metallocene ($\text{TM}(\text{C}_5\text{H}_5)_2$, TM = Fe, Cr and Ni) and the sulfur powder were firstly mixed in an argon filled glove box, then sealed in a quartz tube (φ 8 mm \times 150 mm) under vacuum. The sealed tube was kept at 650 °C for 6 h with a ramp of 5 °C min⁻¹. After cooling down, the resulted TMS@C powders were collected and rinsed with carbon disulfide (CS_2) to remove the unreacted sulfur. Note that in order to get the influence of the metallocene/sulfur ratio on the final products, we firstly took the ferrocene as an example and tried two different ferrocene/sulfur ratio, namely 1:1 and 1:2, based on the stoichiometry of the expected product of FeS and FeS₂, respectively. However, we obtained the same product, the FeS@C, for such two different ratios confirmed by the XRD pattern as shown in the Fig. S7. This indicates that the excess sulfur does not

influence the final products of the FeS@C and only the thermodynamically stable phase corresponding to the reaction condition can be obtained. Then for the other two samples (Cr₂S₃@C and NiS₂@C), we use the same molar ratio of 1:2 to ensure the complete sulfuration of the pyrolyzed products of the metallocene. Furthermore, in order to understand the reaction process, a controlling experiment of FeS@C nanocomposites synthesized at a lower temperature of 450 °C was performed.

Physicochemical characterization The phase structure of the as-prepared TMS@C nanocomposites was identified by a Bruke D2 diffractometer. The morphology characterization was performed on a field emission scanning electron microscope (SEM, FEI Magellan 400). The transmission electron microscopy (TEM) images, and high-resolution TEM (HRTEM) images were collected on a FEI Tecnai™ G2 F20 with an accelerating voltage of 200 kV.

Electrochemical measurements The TMS@C anodes were prepared by mixing the TMS@C powders with Super P carbon and polyvinylidene fluoride (PVDF) in a weight ratio of 80:10:10. The CR2025 coin-type cells were assembled in an argon-filled glove box (M-braun), using the pure lithium metal as anode, 1 M LiPF₆ dissolved in 1:1 (wt) mixture of ethylene carbonate (EC) and diethyl carbonate (DEC) as electrolyte and glass fiber (Whatman, GF/B) as separator. The test cells were galvanostatically cycled in the voltage range of 0.01 V to 3.0 V (versus Li⁺/Li) at room temperature on a program-controlled test system (LAND CT2001A). The specific capacity for the TMS@C anode was calculated based on the weight of the active materials. The cyclic voltammetry (CV) measurements were carried out with a scan rate of 0.1 mV s⁻¹ on an Autolab electrochemical workstation (PGSTAT302N). For *ex situ* SEM, TEM and HRTEM analysis, the cycled anodes were disassembled from the batteries and washed with DEC in argon-filled glove box.

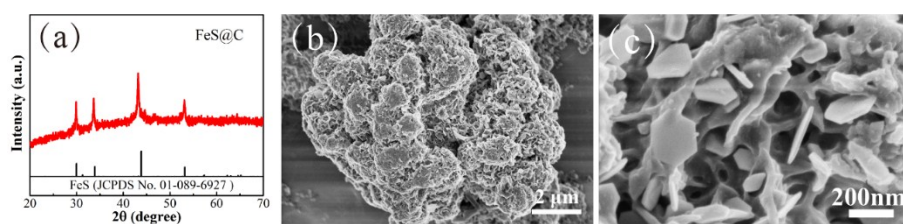


Figure S1 XRD pattern and SEM images for the FeS@C synthesized at 450 °C

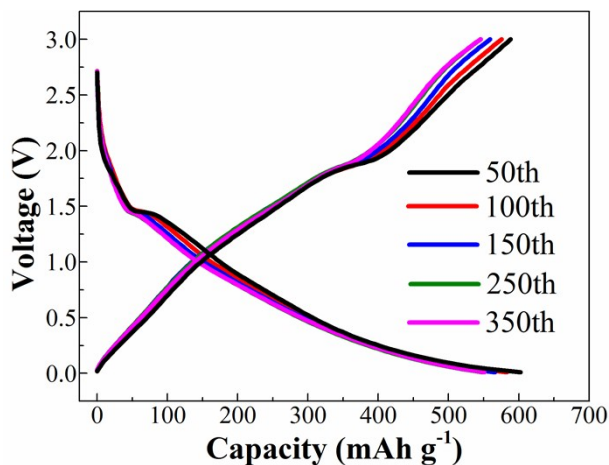
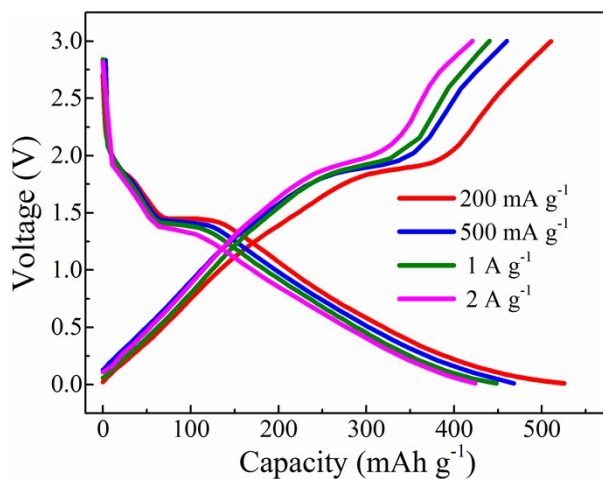


Figure S2 Cycling performance of FeS@C (prepared at 650 °C) with a current density of 100 mA g⁻¹. The discharge-charge profiles for each cycle remain unchanged, indicating a superior stability on cycling.



FigureS3 The discharge-charge profiles of FeS@C (prepared at 650 °C) cycled at different current density.

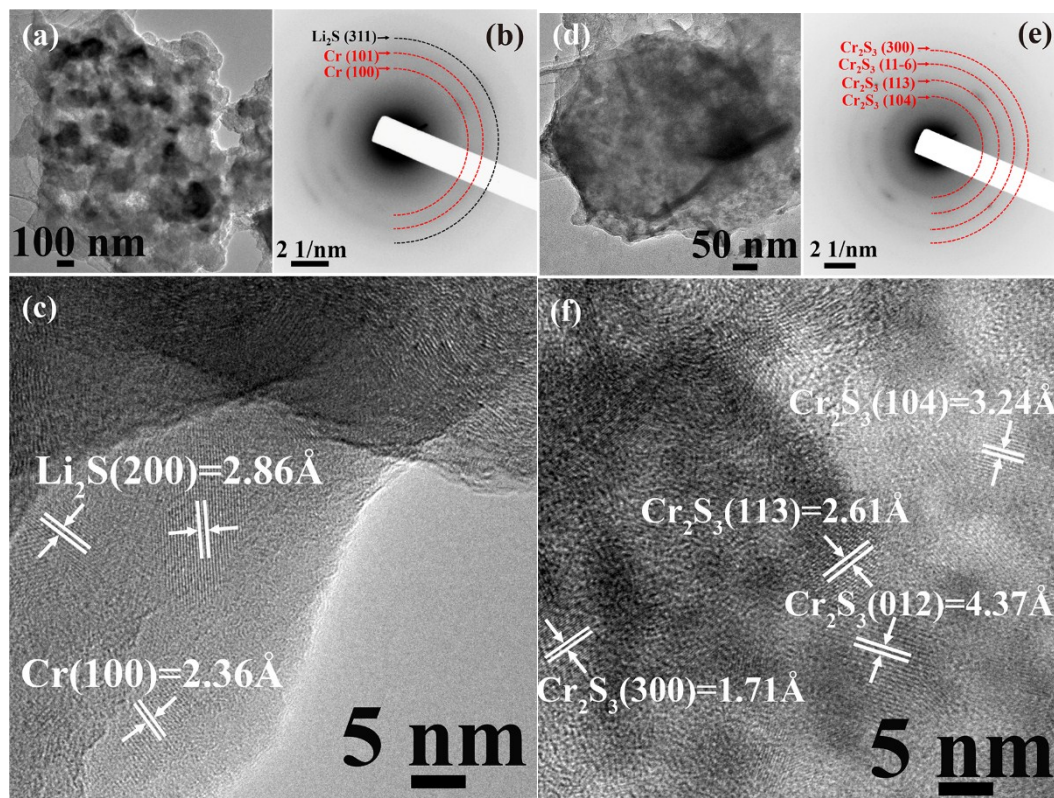


Figure S4 *ex situ* TEM analyses for the $\text{Cr}_2\text{S}_3@\text{C}$ electrode: (a) TEM, (b) SAED and (c) HRTEM of the 2nd discharged electrode; (d) TEM, (e) SAED and (f) HRTEM of the 2nd charged electrode. These results demonstrate that the $\text{Cr}_2\text{S}_3@\text{C}$ electrode are cycled based on the reversible reaction of $\text{Cr}_2\text{S}_3 + 6(\text{Li}^+ + \text{e}^-) = 2\text{Cr} + 3\text{Li}_2\text{S}$.

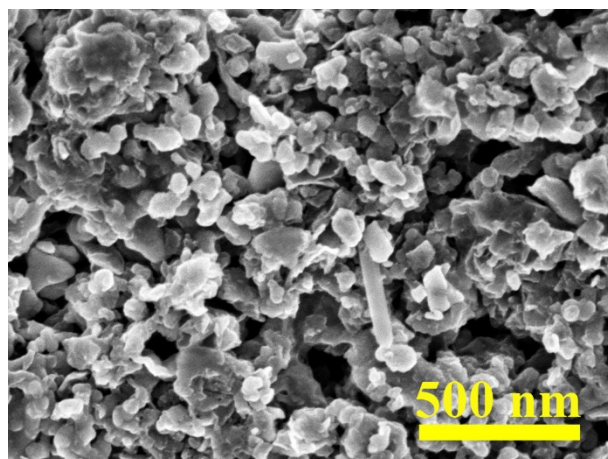


Figure S5 SEM image of the fresh FeS@AC electrode.

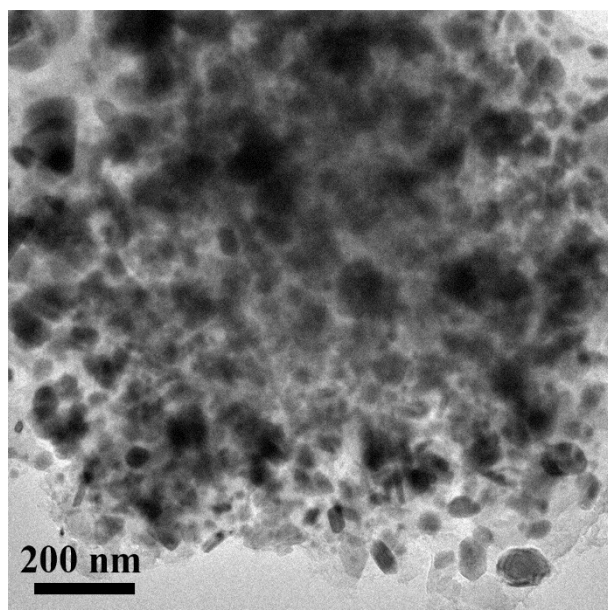


Figure S6 TEM image of the FeS@C prepared at 650 °C, indicating that most of the pristine FeS particles are with a size ranged from 20 to 50 nm.

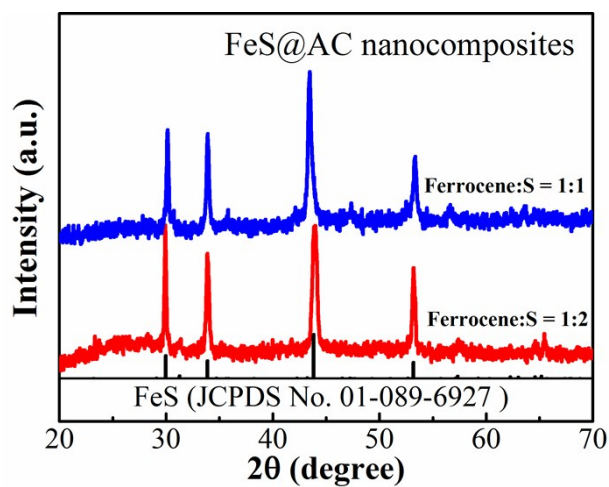


Figure S7 XRD patterns of the product with different ferrocene/S ratio, indicating that the obtained product is the same FeS@C for both the two different ferrocene/S ratio.

Table S1 Comparison of the performance of FeS@C reported in this paper with that of some previously reported FeS-based electrode.

Samples	Synthesis method	Current density (mA g⁻¹)	Capacity (mAh g⁻¹) [cycle number]	Reference
C@FeS nanosheets	Solution-based synthesis method	100	615[100]	[1]
FeS@RGO	Solvent precipitation	100	978[40]	[2]
FeS microsheet	Solution-based approach	100	697[20]	[3]
FeS/carbon nanosheets	Freeze-drying/ carbonization approach	1000	703[150]	[4]
FeS/carbon nanofiber	Electrospinning method	500	475[320]	[5]
Nickel plated FeS powder	-	100	487[30] (0.8-3 V)	[6]
FeS Nanodots in Porous Graphitic Carbon Nanowires	Electrospinning technique	304	~400[50] (1-3 V)	[7]
Carbon-coated FeS on carbon cloth films	Hydrothermal method	92 (0.15C)	~ 420[100] (1-2.6 V)	[8]
FeS nanosheets	Hydrothermal method	100	176[50]	[9]
Graphene-wrapped FeS-graphene nanoribbons	Solution method	400	536[100]	[10]
FeS embedded carbon microsphere	Solvothermal method	500	521[50]	[11]
FeS@C	Gas-phase reaction	100	550[350]	This work
FeS@C	Gas-phase reaction	500	480[500]	This work

Table S2 Comparison of the performance of NiS₂@C reported in this paper with that of some preciously reported nickel sulfide-based electrode. There are some other nickel sulfides (e.g. Ni₃S₂, Ni₃S₄ and Ni₇S₆) being selected for comparing here, due to the availability of the NiS₂ electrode in previous reports.

Samples	Synthesis method	Current density (mA g ⁻¹)	Capacity (mAh g ⁻¹) [cycle number]	Reference
Ni ₃ S ₂ nanotube	Hydrothermal method	100	766[100]	[12]
Ni ₃ S ₂ @N-G	Pyrolysis method	50	809[150]	[13]
Ni ₃ S ₄ /NG	Hydrothermal method	2816 (4C)	558[100]	[14]
NiS ₂ /graphene	Hydrothermal method	500	810[1000]	[15]
NiS ₂ -graphene/ACT	Heat treatment method	870 (1C)	645[100]	[16]
Ni ₇ S ₆	Spray pyrolysis	1000	472[500]	[17]
NiS nanorod	Solvothermal method	59	887[60]	[18]
NiS ₂ &NiS@C	Hydrothermal method	208	517[50]	[19]
NiS ₂ &NiS@N-doped graphene	Hydrothermal method	50	425[50]	[20]
NiS ₂ @C	Gas-phase reaction	100	670[160]	This work

References:

1. C. Xu, Y. Zeng, X. Rui, N. Xiao, J. Zhu, W. Zhang, J. Chen, W. Liu, H. Tan, H. H. Hng and Q. Yan, *ACS Nano*, 2012, **6**, 4713.
2. L. Fei, Q. Lin, B. Yuan, G. Chen, P. Xie, Y. Li, Y. Xu, S. Deng, S. Smirnov and H. Luo, *ACS Appl. Mater. Interfaces*, 2013, **5**, 5330.
3. C. Xing, D. Zhang, K. Cao, S. Zhao, X. Wang, H. Qin, J. Liu, Y. Jiang and L. Meng, *J. Mater. Chem. A*, 2015, **3**, 8742.
4. Y. Xu, W. Li, F. Zhang, X. Zhang, W. Zhang, C. S. Lee and Y. Tang, *J. Mater. Chem. A*, 2016, **4**, 3697.
5. L. Fei, B. P. Williams, S. H. Yoo, J. M. Carlin and Y. L. Joo, *Chem. Commun.*, 2016, **52**, 1501.
6. S. H. Kim, Y. J. Choi, D. H. Kim, S. H. Jung, K. W. Kim, H. J. Ahn, J. H. Ahn and H. B. Gu, *Surf. Rev. Lett.*, 2008, **15**, 35.
7. C. Zhu, Y. Wen, P. A. van Aken, J. Maier and Y. Yu, *Adv. Funct. Mater.*, 2015, **25**,

- 2335.
8. X. Wei, W. Li, J.-a. Shi, L. Gu and Y. Yu, *ACS Appl. Mater. Interfaces*, 2015, **7**, 27804.
 9. K. Chen, K. Cao, C. Xing, Y. Hu, J. Liu, Y. He, J. Wang, A. Li and H. Qin, *J. Alloys Compd.*, 2016, 688, Part A, 946.
 10. L. Li, C. Gao, A. Kovalchuk, Z. Peng, G. Ruan, Y. Yang, H. Fei, Q. Zhong, Y. Li and J. M. Tour, *Nano Res.*, 2016, DOI: 10.1007/s12274-016-1175-x, 1.
 11. B. Wu, H. H. Song, J. S. Zhou and X. H. Chen, *Chem. Commun.*, 2011, **47**, 8653.
 12. D. Li, X. Li, X. Hou, X. Sun, B. Liu and D. He, *Chem. Commun.*, 2014, **50**, 9361.
 13. J. Zhu, Y. Li, S. Kang, X. L. Wei and P. K. Shen, *J. Mater. Chem. A*, 2014, **2**, 3142.
 14. N. Mahmood, C. Zhang and Y. Hou, *Small*, 2013, **9**, 1321.
 15. Q. Chen, W. Chen, J. Ye, Z. Wang and J. Y. Lee, *J. Power Sources*, 2015, **294**, 51.
 16. Z. Gao, N. Song, Y. Zhang and X. Li, *Nano Lett.*, 2015, **15**, 8194.
 17. M. Y. Son, J. H. Choi and Y. C. Kang, *J. Power Sources*, 2014, **251**, 480.
 18. H. Geng, S. F. Kong and Y. Wang, *J. Mater. Chem. A*, 2014, **2**, 15152.
 19. B. Y. Liu, C. H. Fan, J. W. Chen, Y. Zhou, L. H. Dong, J. H. Wang, *Mater Lett.*, 2015, 142, 90.
 20. H. C. Tao, X. L. Yang, L. L. Zhang, S. B. Ni, *J. Electroanal. Chem.*, 2015, 739, 36.